第 35 卷第 6 期 无 机 化 学 学 报 Vol.35 No.6
2019 年 6 月 CHINESE JOURNAL OF INORGANIC CHEMISTRY 1085-1092

$Sr_{0.955}Al_{2-x}B_xSi_2O_8$:0.025$Eu^{2+}$荧光粉的制备、晶体结构及发光性能

王 飞*,[1,2] 田一光*,[3] 张 乔[3]
([1]安徽三联学院实验中心,合肥 230601)
([2]安徽大学化学化工学院,合肥 230601)
([3]温州大学化学与材料工程学院,温州 325035)

摘要:通过高温固相反应在弱还原气氛下制备了 $Sr_{0.955}Al_{2-x}B_xSi_2O_8$:0.025$Eu^{2+}$($x$=0~0.9)一系列荧光粉,研究了 B(Ⅲ)取代基质晶格中的 Al(Ⅲ)对荧光粉晶体结构和 Eu^{2+}发光性能的影响。B(Ⅲ)以类质同相取代基质晶格中 Al(Ⅲ),形成了连续固溶体。随着 B(Ⅲ)取代量的增加,荧光粉的晶胞参数(a、b、c)和晶胞体积(V)呈线性递减,而晶胞参数(β)呈线性递增。荧光粉的激发光谱为位于 225~400 nm 的宽峰,表观峰值位于 350 nm,激发峰的半高宽(FWHM)随着 B(Ⅲ)取代量的增加,从 90 nm 减小到 102 nm。发射光谱位于 370~600 nm 的宽峰,可拟合为 409 和 447 nm 两个峰,表观峰值位于 409 nm。随着 B(Ⅲ)取代量的增加,2 个拟合峰位均出现蓝移且 2 个峰强度比呈线性递减。根据试样荧光光谱,通过 Van Uitert 经验公式计算得出 $SrAl_2Si_2O_8$:Eu^{2+}中 Sr^{2+}的配位数为 9。随着 B(Ⅲ)取代 Al(Ⅲ)进入基质晶格,造成发光中心 Eu 与配体 O 距离增加,使得 Eu^{2+}所处的晶体场强度减小,发光中心 Eu^{2+}的 5d 能级分裂减小,造成 Eu^{2+}最低发射能级重心上移,2 个拟合谱峰峰位均呈线性蓝移。

关键词:荧光粉;$SrAl_2Si_2O_8$:Eu^{2+};硼置换;晶体结构;光谱特性
中图分类号:O614.37+1;O614.33+8;O613.72 **文献标识码**:A **文章编号**:1001-4861(2019)06-1085-08
DOI:10.11862/CJIC.2019.126

Synthesis, Crystal Structure and luminescent Properties of $Sr_{0.955}Al_{2-x}B_xSi_2O_8$:0.025$Eu^{2+}$ Phosphors

WANG Fei*,[1,2] TIAN Yi-Guang*,[3] ZHANG Qiao[3]
([1]*Experimental Center of Anhui Sanlian University, Hefei* 230601, *China*)
([2]*College of Chemistry and Chemical Engineering, Anhui University, Hefei* 230601, *China*)
([3]*College of Chemistry and Materials Engineering, Wenzhou University, Wenzhou, Zhejiang* 325035, *China*)

Abstract: A series of luminescence phosphors $Sr_{0.955}Al_{2-x}B_xSi_2O_8$:0.025$Eu^{2+}$ (x=0~0.9) were prepared via solid-state reaction in a weak reductive atmosphere. The lattice positions and the luminescent mechanism of Eu^{2+} in the host were discussed, the effects of B(Ⅲ)-substitution on the host lattices and spectral properties were also investigated. It was found that the complete solid solutions were formed in the whole range of x=0~0.9, as B(Ⅲ) substituted for Al(Ⅲ) entered to $SrAl_2Si_2O_8$. The lattice parameters (a, b, c) and unit cell volume (V) of phosphors $Sr_{0.955}Al_{2-x}B_xSi_2O_8$:0.025$Eu^{2+}$ (x=0~0.9) decreased linearly and lattice parameter (β) increased linearly as the increase of substitution amount of B(Ⅲ). A broad excitation spectrum consisted of four excitation bands, which was in a range of 225~400 nm, and an apparent peak at 350 nm. Full width at half maximum (FWHM) increased from 90 to 102 nm as increase of the substitution amount of B(Ⅲ). The emission spectrum was a broad-band in a range of 370~600 nm,

收稿日期:2018-12-27。收修改稿日期:2019-04-10。
国家自然科学基金(No.20771086)、安徽省教育厅重点项目(No.KJ2016A893)、安徽省高校优秀青年人才支持计划项目(No.gxyq2018126)、安徽三联学院科研项目(No.KJZD2018004,2015Z001,2013Z001)、安徽三联学院质量工程项目(No.15zlgc008,16zlgc060,17zlgc030)和国家级大学生创新创业项目(No.201710959055,201710959074,2018109050)资助。
*通信联系人。E-mail:wangfchina@163.com,gytian@wzu.edu.cn;会员登记号:S06N0267M1705。

which could be fitted two peaks of 409 and 447 nm, and its apparent peak was at 409 nm. Two fitted peaks were blue shifted and the intensity ratio of the fitted peaks decreased linearly as the increase of the substitution amount of B(Ⅲ)). The coordination number of Sr^{2+} was 9 in $SrAl_2Si_2O_8:Eu^{2+}$, which has been confirmed by the experimental results and empirical formula of Van Uitert. The distance between the luminescent center Eu and the ligand O increased due to the Al(Ⅲ) replaced by B(Ⅲ), so that the crystal field strength of Eu^{2+} decreased, and the 5*d* energy level split of the luminescent center Eu^{2+} decreased, the center of gravity of the lowest emission level of Eu^{2+} was shifted upward, and the two fitted peaks were linearly blue-shifted.

Keywords: luminescence; $SrAl_2Si_2O_8:Eu^{2+}$; B(Ⅲ)-substitution; crystal structure; luminescent properties

0 Introduction

Since the advent of high-brightness Blu-ray emitting light-emitting diodes (blue-LEDs)[1], the efficacy of white light-emitting diode lamps (WLEDs, also called LEDs) based on InGaN blue chip and phosphor package has surpassed that of incandescent lamps[2]. In the fields of flashlights, desk lamps, traffic lights, signs, decorations, display backlights, *etc*., traditional incandescent and cathode fluorescent lamps have begun to be replaced by LEDs[3-5]. Currently, the most common LED type is "fluorescence conversion" (pc-WLED), due to the low cost, simple structure, uniform performance and easy commercialization. pc-WLEDs will become an indispensable part of the next-generation lighting industry and display system. High-light color stability of phosphor materials has become a new challenge for researchers as the development of low-cost, high-efficiency and high-color rendering[6-8]. Silicates as a phosphor matrix, which can be excited by near-ultraviolet LED chips, have advantages of high energy efficiency, stable physicochemical properties, cheap and easy to obtain raw materials. Therefore, silicate-based phosphors have become a research hotspot[9-14]. $SrAl_2Si_2O_8$ is a framework-like aluminosilicate structure in which silicon (aluminum) oxygen tetrahedrons are connected in a three-dimensional space in a common angular manner, and alkaline earth metal ions present in the voids of the skeleton [15]. Recently, the main research focuses on the modulation of fluorescence spectra by adjusting the cation composition in the matrix. The emission peak of Eu^{2+} is linearly red shifted, as Ti^{4+} substituted for Si^{4+} in $CaAl_2Si_2O_8$[16]. The researchers obtained a series of promising cyan, green, and yellow emission $(Ba,Sr)_3(Si,Al)_6(O,N)_{15}:Eu^{2+}$ phosphors by changing Sr^{2+} to Ba^{2+}, Al^{3+} to Si^{4+} and N^{3-} to O^{2-}[17]. However, little research has been conducted on the changes in crystal structure and spectral changes caused by the changes in skeleton ions in the phosphor matrix.

In this work, a series of $Sr_{0.955}Al_{2-x}B_xSi_2O_8:0.025Eu^{2+}$ (x =0 ~0.9) samples were designed and synthesized. According to the X-ray powder diffraction data of the samples, the crystallographic parameters of the samples were calculated by Maud (2.14) software full-spectrum fitting method, and the fluorescence spectrum of the samples were fitted by Gaussian function with Origin 7.5 software. The correlation effect of B(Ⅲ) substituted for Al(Ⅲ) on its crystal structure and spectral changes were discussed.

1 Experimental

1.1 Synthesis

We synthesized a series of phosphors based on the chemical composition of $Sr_{0.955}Al_{2-x}B_xSi_2O_8:0.025Eu^{2+}$, in which x indicated the B(Ⅲ) concentration. The raw materials were $SrCO_3$ (AR), H_3BO_3 (GR), $Al(OH)_3$ (AR), H_2SiO_3 (AR), and Eu_2O_3 with a purity of 99.99%. The raw materials were thoroughly mixed with $n_{Sr}:n_{Al}:n_B:n_{Si}:n_{Eu}=0.955:(2-x):x:2:0.025$ in an agate mortar by grinding and then placed in a corundum crucible with a lid. Then the mixture was preheated at 1 000 ℃ to the sufficient diffuse and infiltration, with a soaking time of 2.5 h in CO reducing atmosphere, meanwhile, carbon grains were used as a reducing agent and

covered the samples during firing. Subsequently, the preheated mixtures were milled sufficiently again after cooling and sintered at 1 200 ℃ for 4 h in CO reducing atmosphere.

1.2 Characterization

The powder X-ray diffraction (XRD) patterns were collected with Bruker D8 advance diffractometer (Cu $K\alpha_1$, λ=0.154 06 nm), in a Bragg-Brentano reflection geometry with a Sol-X detector over the scattering angle range of $10° \leqslant 2\theta \leqslant 90°$, a step of 0.02°, a potential of 40 kV, a current of 40 mA, and a scan speed of 0.12°·min^{-1}. The Rietveld refinement against XRD data was fitted by the Maud (2.14) program. The measurements of photo luminescence were performed by FluoroMax-4 (HORIBA JobinYvon) using a Xe flash lamp with a scan speed of 1 nm·s^{-1}. All of the characterizations were conducted at room temperature.

2 Results and discussion

2.1 XRD analysis

XRD patterns of the samples are shown in Fig.1. All the peaks could be indexed to $SrAl_2Si_2O_8$ phase according to PDF No.38-1454, which indicated that single-phase $SrAl_2Si_2O_8$:Eu^{2+} phosphors were obtained, and the co-doped Eu^{2+} and B(Ⅲ) ions did not form a new phase besides the host materials. $SrAl_2Si_2O_8$ belongs to monoclinic system (space group $C2/m$(12)). The peaks of the ($\bar{1}$12), ($\bar{2}$20), (002) and (041) planes shifted to higher angles as the increase of B(Ⅲ) (Fig.2), which might be ascribed to the smaller radius of B(Ⅲ) (0.023 nm) than Al(Ⅲ) (0.051 nm)[18]. When Al were occupied the B sites in the host, the smaller radius result in smaller crystal plane spacing d. According to the Bragg equation:

$$2d\sin\theta = n\lambda \quad (1)$$

In the Formula (1), d is the inter planar spacing, θ is the diffraction peak angle, n is the diffraction order, and λ is the wavelength of the X-ray. The values of $d_{(\bar{1}12)}$, $d_{(\bar{2}20)}$ and $d_{(002)}$ decreased linearly as the increase of the substitution amount of B(Ⅲ) (Fig.2 and 3). In addition, the non-crystalline content of samples increased as the increase of the substitution amount of B(Ⅲ) (Fig.1). Topas3 software was used to calculate the XRD data of the samples, and the results show that the crystallinity of the samples were gradually decreased after the addition of B(Ⅲ), indicating the glass samples were generated with the increase of the boron (Fig.4). The crystallinity of the sample with x=0.9 was reduced

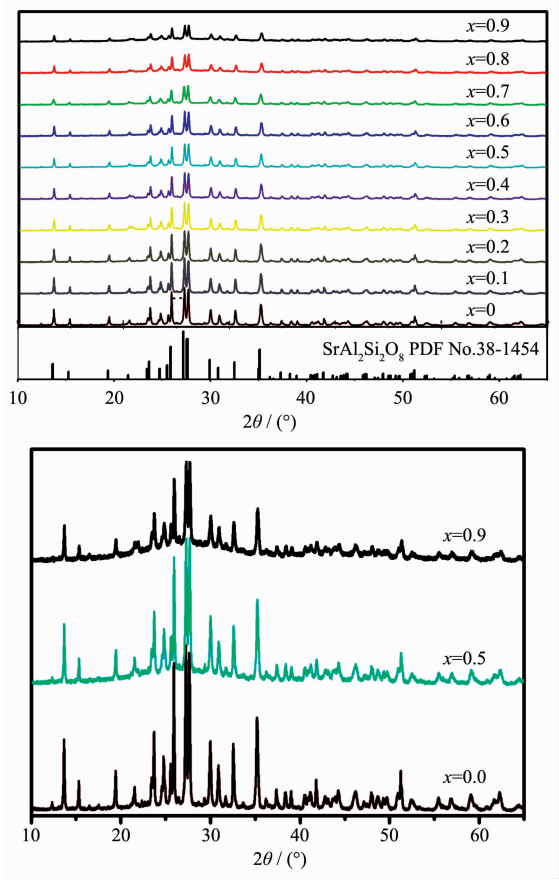

Fig.1 XRD patterns of $Sr_{0.955}Al_{2-x}B_xSi_2O_8$:0.025$Eu^{2+}$ (x=0~0.9) phosphors

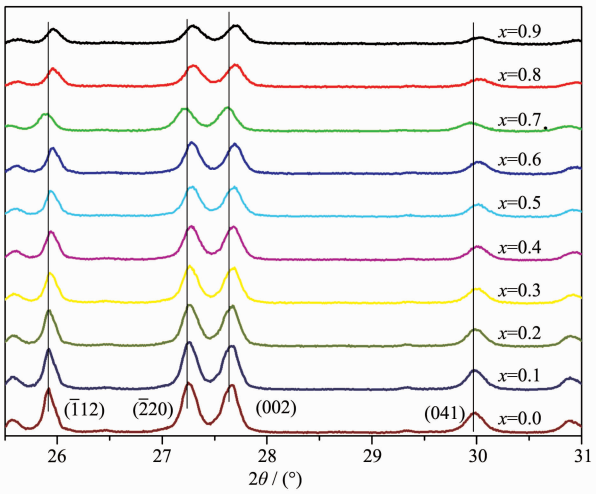

Fig.2 XRD patterns of $Sr_{0.955}Al_{2-x}B_xSi_2O_8$:0.025 Eu^{2+} (2θ=25.5°~31°) phosphors

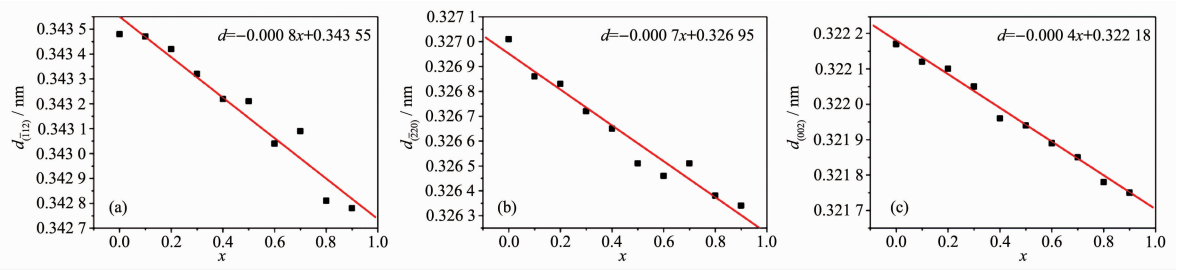

Fig.3 (a) $d_{(\bar{1}11)}$, (b) $d_{(\bar{2}20)}$ and (c) $d_{(002)}$ of $Sr_{0.955}Al_{2-x}B_xSi_2O_8$:0.025$Eu^{2+}$ (x=0~0.9) phosphors varied with x

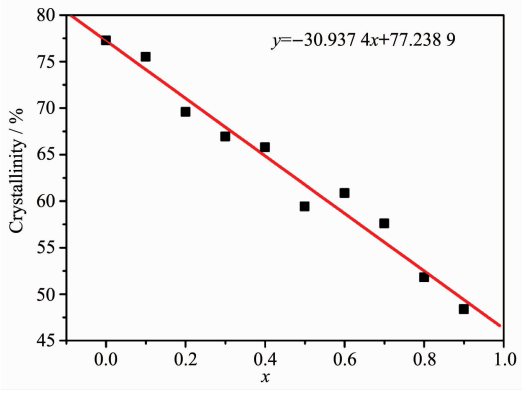

Fig.4 Crystallinity of $Sr_{0.955}Al_{2-x}B_xSi_2O_8$:0.025$Eu^{2+}$ (x=0~0.9) phosphors varied with x

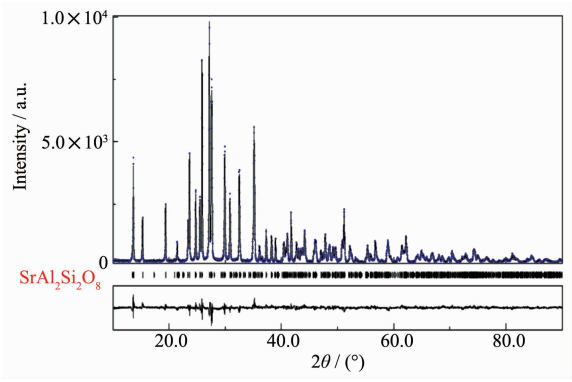

Fig.5 Observed (blue dashed line) and calculated (black line) XRD patterns of $Sr_{0.955}Al_2B_{0.1}Si_2O_8$:0.025$Eu^{2+}$ as well as the difference profile (bottom line) between them; Bragg reflection peak positions are shown as vertical bars; An ideal crystal structure is also shown in the inset

by 37.4% compared to the sample with x=0.

The grain size of each powder sample was calculated by the Scherrer formula from the half width of the diffraction peak at 2θ=27.248° of the sample:

$$L=K\lambda/(W\cos\theta) \quad (2)$$

In the Formula (**2**), L (nm) is the grain size in the direction perpendicular to the emitting surface (hkl); K is Scherrer constant, and the value is 0.89; W (rad) is FWHM of the sample diffraction peak. The value of W of the sample with x=0 is 0.005 2 rad, and the value of each parameter was brought into the Formula (**2**) which calculated that L is 46.004 4 nm; when x=1.0, W of the sample is 0.004 1 rad and the calculated L is 33.520 2 nm. The calculation results show that the grain size of the sample decreased as the increase of the substitution amount of B(Ⅲ).

Cell dimensions of the compositions in the system were calculated by the full pattern fitting method (Fig. 5). The crystal structure refinement of $Sr_{0.955}Al_{1.9}B_{0.1}Si_2O_8$:0.025$Eu^{2+}$ was done by taking $SrAl_2Si_2O_8$ as the starting model with space group $I2/c$[19]. The observed, calculated, and difference patterns are shown in Fig.6. Additionally, the calculated residual factor values R_{wp}, R_{exp} and sig were 6.20%, 8.16%, 4.95% and 1.68, respectively, indicating good refinement quality.

According to XRD patterns of the samples, both the lattice parameters (a, b, c, β) and unit cell volume (V) of $Sr_{0.955}Al_{2-x}B_xSi_2O_8$:0.025$Eu^{2+}$ (x=0~0.9) phosphors were calculated by the full pattern fitting method. It shows that the a, b, c and V of $Sr_{0.955}Al_{2-x}B_xSi_2O_8$:0.025$Eu^{2+}$ (x=0~0.9) phosphors decreased linearly, and β increased linearly with the increase of x (Fig.6), which may be attributed to the smaller radius of B(Ⅲ) than Al(Ⅲ) It could be further explained that the Al(Ⅲ) were occupied by the B(Ⅲ) site in the host which was benefit to reduce the volume from [AlO_4] to [BO_4], thus resulting in a decrease in unit cell parameters and volume. However, the change rate and variable quantity of lattice parameters are not consistent (Fig. 6). With the substitution amount of B(Ⅲ) increased from 0 to 0.9, the parameters a, b, c and V decreased by 0.000 9, 0.002 1 and 0.002 5 nm, respectively. The variation range of c is significantly larger than a

and b. β increased linearly with the increase of x.

According to the standard crystal structure model data of $SrAl_2Si_2O_8$[19], the structure diagram was made by using Diamond (3.1) software. In $SrAl_2Si_2O_8$, the silicon (aluminum) tetrahedra constituted the skeleton of a, b plane direction along the c-axis layering. Sr^{2+} ions arranged between the skeleton layers (Fig.7). It could be seen that the density of aluminum tetrahedron arranged on the c-axis direction was the highest, and that arranged on the b-axis was followed and a-axis was minimum. Therefore, the variation range of c was significantly larger than a and b as the increase of x. The (001) and (100) crystal plane constituted the crystal plane angle (β). The difference of change rate

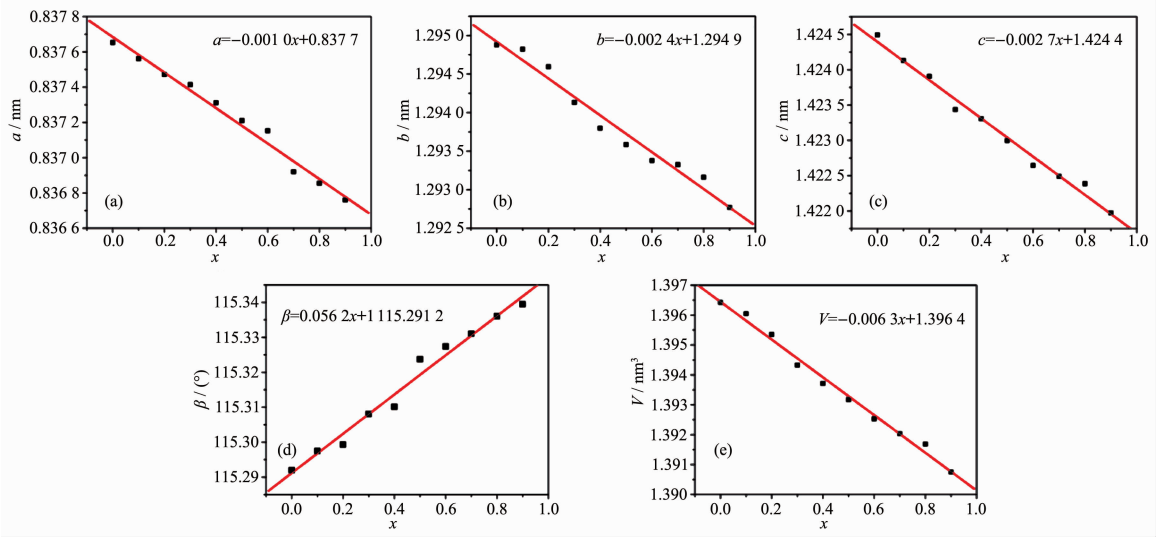

Fig.6　Lattice parameters and unit cell volumes of $Sr_{0.955}Al_{2-x}B_xSi_2O_8$:0.025$Eu^{2+}$ (x=0~0.9) phosphors varied with x

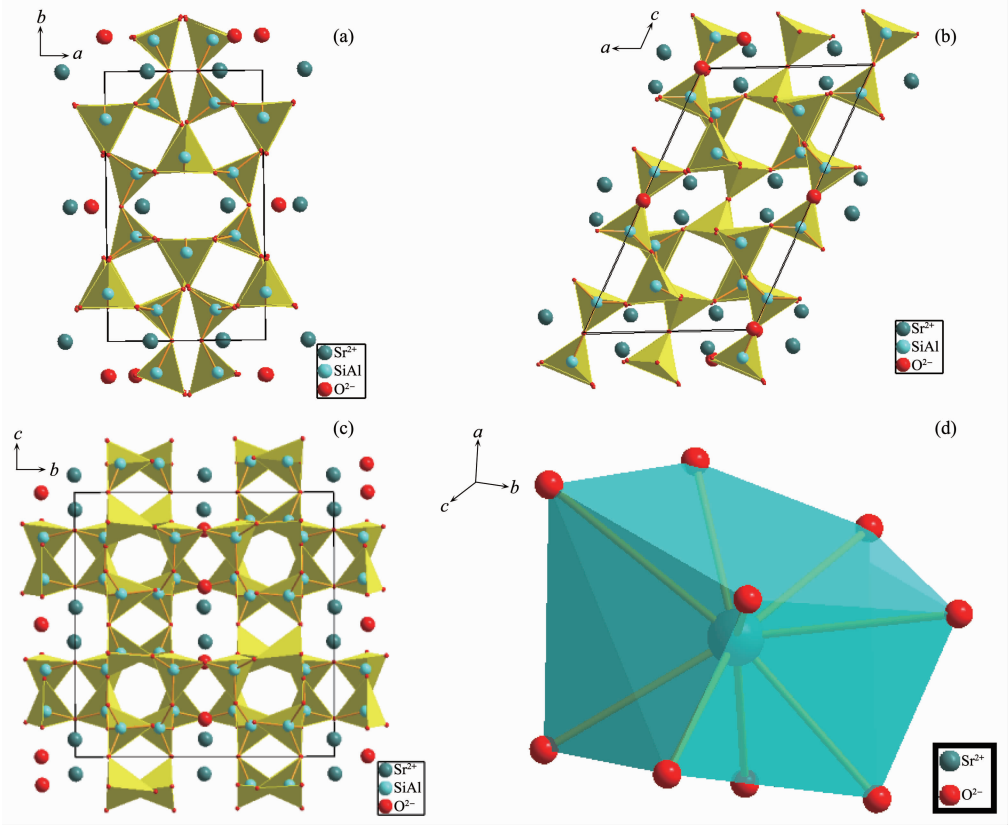

Fig.7　Illustrations of crystal structures of $SrAl_2Si_2O_8$

between the *a*-axis and *c*-axis caused the amplitude of the (001) plane changed to be larger than (100) plane, resulting in the increase of β.

2.2 Fluorescence spectra analysis

The excitation spectrum of $Sr_{0.955}Al_{2-x}B_xSi_2O_8$: $0.025Eu^{2+}$ located around 225~400 nm. The maximum emission wavelength located at 350 nm and FWHM was 90 nm. The four excitation peaks (270, 314, 340 and 364 nm) when x=0 were fitted by Gauss. With the substitution amount of B(Ⅲ) increased from 0 to 0.9, the positions of the fitted peaks at 270 and 314 nm remained unchanged, however, the peak intensity decreased at 270 nm and increased at 314 nm. The excitation peaks at 340 and 364 nm showed clear blue-shift. The peak intensity increased at 340 nm and significantly reduced at 364 nm, making the apparent excitation peak width at half maximum increased to 102 nm (Fig.8).

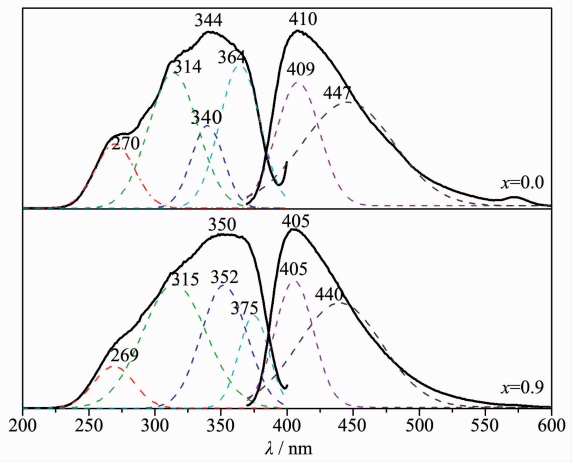

Fig.8 Luminescence spectra of $Sr_{0.955}Al_{2-x}B_xSi_2O_8$:$0.025Eu^{2+}$

Luminous characteristics of Eu^{2+} was studied in the sulfides, halides and aluminate matrix by Van Uitert[20]. Studies have shown that the 5*d* excited state band edge of Eu^{2+} has an effect on its coordination number, and the empirical formula is as follow:

$$E=Q[1-(V/4)^{1/V}10^{-nrE_A/80}] \quad (3)$$

Equation (**3**) was taken the logarithm of both sides of Equation (**4**):

$$nr=-(80/E_A)\lg[(1-E/Q)(V/4)^{-(1/V)}] \quad (4)$$

where E represents the position of the *d*-band edge in energy for the rare-earth ion (cm^{-1}), here, the emission peak of Eu^{2+} is 410 nm, so E is 24 390 cm^{-1}; Q represents the position of the lower *d*-band edge in energy for the free ion, Q is 34 000 cm^{-1} for Eu^{2+}; V is the valence of the 'active' cation, here Eu^{2+} as the activator ions, so V is 2; E_A (eV) is the electron affinity of the atoms that form anions. Van Uitert's research shows that the value of E_A is related to the type of coordination ion, and when the species of coordination ions are different, E_a is the smaller in the coordination ions. The E_A of simple compounds of oxygen is 1.17 eV, and the E_A of $Y_3Al_5O_{12}$ and $GdAlO_3$ aluminate system is 1.60 eV. E_A increased as the increase of the amount of charge in the central atom in the oxyanion group. For example SiO_4^{4-}, PO_4^{3-} and WO_4^{2-} have higher E_A values. Because $SrAl_2Si_2O_8$ belongs to aluminum silicate system, in which the Sr^{2+} taken by the activator has two ligands, silicate and aluminate, E_A value is 2.65 eV. In the crystal, n is the number of coordinated anions and r is the radius of the host cation replaced by the 'active' cation. The above-mentioned parameter values were brought into the Equation (**4**): nr=1.227 0, the nine-coordinated Sr^{2+} ion radius is 0.131 nm and the calculated coordination number is 9.36, which can be inferred that Sr^{2+} is nine-coordinated in $SrAl_2Si_2O_8$.

The emission spectrum, which was also a broad-band between 370 and 600 nm, could be fitted by two peaks at 409 and 447 nm, and its apparent peak located at 409 nm. The apparent peak was blue-shifted from 410 to 405 nm as well as the two fitted apparent peaks were blue-shifted linearly with the increase of the substitution amount of B(Ⅲ), and the slopes of the lines are −3.944 0 and −6.814 3, respectively (Fig.9). The emission peak area of luminescence center Eu^{2+}_1 in 409 nm (A_{Em1}) and the emission peak area of luminescence center Eu^{2+}_2 in 447 nm (A_{Em2}) decreased linearly with the increase of the amount of the substitution amount of B(Ⅲ) (Fig.10). The rate of change of the displacement and intensity of the fitted peak at 447 nm was larger than at 409 nm, indicating that B(Ⅲ) entered into the lattice and has a greater impact on the luminescence centers at 447 nm. When the substitution amount of B(Ⅲ) was 1.0, two fitting peak positions were blue-shifted to 405 and 440 nm, and FWHM reduced from 74 to 65 nm.

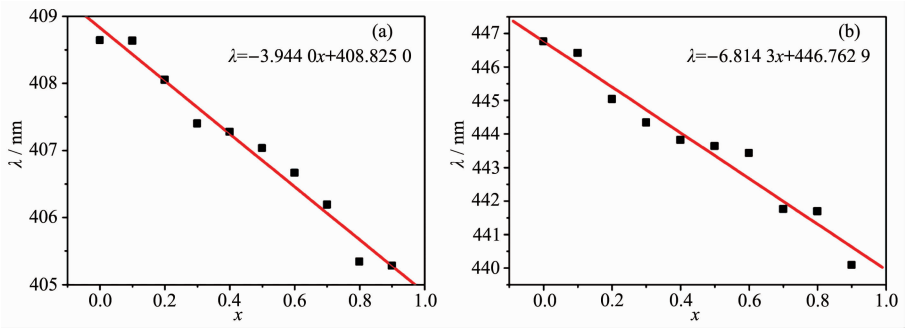

(a) Relationship between peak position of short-wavelength fitting peak and the substitution amount of B(Ⅲ);
(b) Relationship between peak position of long-wavelength fitting peak and the substitution amount of B(Ⅲ)

Fig.9　Relationship between spectra position of Gaussian fitted and the substitution amount of B(Ⅲ)

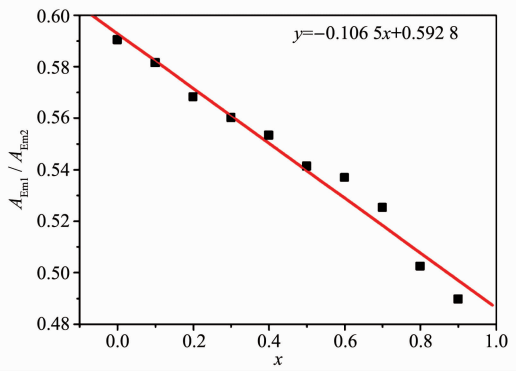

Fig.10　Area ratio of emission spectra from two luminescent centers vared with the substitution amount of B(Ⅲ)

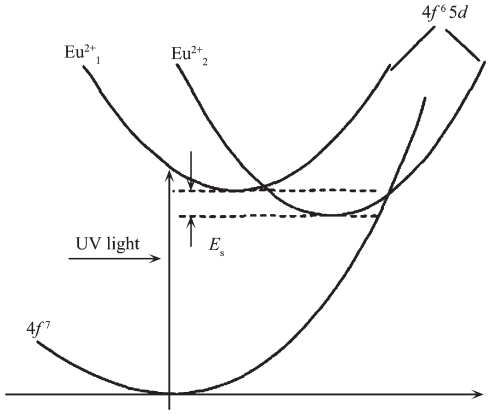

Fig.11　Configuration coordination model for the Eu^{2+}_1 and Eu^{2+}_2 sites in the $SrAl_2Si_2O_8$:Eu^{2+}

2.3　Luminescence mechanism of Eu^{2+}

The luminescence mechanism of Eu^{2+} in the matrix crystal $SrAl_2Si_2O_8$ can be well illustrated by the bit-shaped coordinate model diagram. The luminescence of Eu^{2+} is mainly due to the transition of $4f^65d \rightarrow 4f^7$ electrons. Since Eu^{2+} entered the $SrAl_2Si_2O_8$, two different energy levels of $4f^65d$ were formed, resulting in the existence of two different luminescent centers of Eu^{2+}_1 and Eu^{2+}_2 in the phosphor $SrAl_2Si_2O_8$:Eu^{2+}. Therefore, when the electrons transfered from the excited state back to the ground state level, the energy released was different, and the wavelength at which the fluorescence was generated was different. Eu^{2+}_1 was in a higher excited state energy position and produced a short wavelength emission of 406 nm; Eu^{2+}_2 was in a position with low excited state energy and produced a long wavelength emission of 447 nm (Fig.11). E_s is the energy difference between the lowest energy levels of Eu_1^{2+} and Eu_2^{2+}.

The $4f^65d$ configuration of Eu^{2+} electrons was formed by the strong coupling of $4f$ and $5d$ electrons under the action of electrostatic force. The $5d$ electrons of Eu^{2+} did not have shielding effect and were in a bare state, so they were sensitive to the changes in the surrounding crystal field environment[21]. With the increase of the substitution amount of B(Ⅲ), the number of titanium oxide tetrahedrons [BO_4] formed in the matrix crystal gradually increased, because the volume of titanium oxide tetrahedron [BO_4] is smaller than that of the silicon tetrahedron [AlO_4]. The gap between the tetrahedrons increased, and the distance between the luminescence center Eu^{2+} in the gap and the ligand tetrahedron became larger. According to the fifth power of the crystal field intensity (D_q) around Eu^{2+} and the distance (R) from Eu^{2+} to O, the D_q of Eu^{2+} was weakened and the $5d$ energy level splitting became smaller[22], making the lowest emission level of Eu^{2+} shifted downward. The center of gravity of the emission level

shifted upward, resulting in a blue shift of the two fitted peaks of the $4f^6 5d \rightarrow 4f^7$ emission band of the luminescence center Eu^{2+}.

3 Conclusions

The complete solid solutions were formed in the whole range of x=0~0.9, as B(Ⅲ) substituted for Al(Ⅲ) entered to $SrAl_2Si_2O_8$. The lattice parameters (a, b, c) and unit cell volume (V) of $Sr_{0.955}Al_{2-x}B_xSi_2O_8$:0.025$Eu^{2+}$ (x =0 ~0.9) phosphors decreased linearly, the crystal plane spacing ($\bar{1}12$), ($\bar{2}20$), (002)) and lattice parameter (β) increased linearly with the increase of the substitution amount of B(Ⅲ).

The broad-band excitation spectrum of the samples could be fitted to four peaks which were in the range of 225 ~400 nm, and the apparent peak was around 350 nm. The emission spectrum was a broad-band in the range of 370 ~600 nm, which could be fitted by two peaks at 409 and 447 nm, and its apparent peak was at 409 nm, FWHW was 74 nm, and Sr^{2+} was nine-coordinated in $SrAl_2Si_2O_8$. As the substitution amount of B(Ⅲ) increased, the center of gravity of the emission level shifted upward, resulting in a blue shift of the two fitted peaks of the $4f^6 5d \rightarrow 4f^7$ emission band of the luminescence center Eu^{2+}, and FWHW was reduced from 74 to 65 nm.

Acknowledgements: This study was supported by the National Natural Science Foundation of China (Grant No. 20771086), the Key projects of the Department of Education of Anhui Province (Grant No.KJ2016A893), the Support Project for Outstanding Young Talents in Colleges and Universities of Anhui Province (Grant No.gxyq2018126), the Scientific Research Project of Anhui Sanlian University (Grant No.KJZD2018004, 2015Z001, 2013Z001), the Quality Engineering Project of Anhui Sanlian University (Grant No.15zlgc008, 16zlgc060, 17zlgc030), and the National College Students Innovation and Entrepreneurship Training Program (Grant No.201710959055, 201710959074, 2018109050).

References:

[1] Nakamura S, Mukai T, Senoh M. *Appl. Phys. Lett.*, **1994**,**64**: 1687-1689

[2] Ci Z P, Que M D, Shi Y R, et al. *Inorg. Chem.*, **2014**,**53**: 2195-2199

[3] Xia Z G, Liu Q L. *Prog. Mater. Sci.*, **2016**,**84**:59-117

[4] Lin C C, MeijerinkA, Liu R S. *J. Phys. Chem. Lett.*, **2016**,**7**: 495-503

[5] Zhong J S, Chen D Q, Yuan S, et al. *Inorg. Chem.*, **2018**,**57**: 8978-8987

[6] Ye S, Xiao F, Pan Y X, et al. *Mater. Sci. Eng. R*, **2010**,**71**: 1-34

[7] Cai P Q, Qin L, Chen C L, et al. *Inorg. Chem.*, **2018**,**57**: 3073-3081

[8] WANG Fei(王飞). *Acta Photonica Sinica*(光子学报), **2018**, **47**(8):0816001

[9] Ray S, Tadge P, Nair G B, et al. *Ceram. Int.*, **2018**,**44**:5506-5512

[10]Homayoni H, Sahi S, Ma L. *J. Lumin.*, **2018**,**198**:132-137

[11]Tang Z B, Wang D Y, Khan W U, et al. *J. Mater. Chem. C*, **2016**,**4**:5307-5313

[12]Kalaycioglu N O, Circir E. *J. Therm. Anal. Calorim.*, **2013**, **111**:273-277

[13]Hai O, Jiang H Y, Xu D, et al. *Mater. Res. Bull.*, **2016**,**76**: 358-364

[14]Yang W J, Luo L Y, Chen T M, et al. *Chem. Mater.*, **2005**, **17**:3883-3888

[15]Clabau F, Garcia A, Bonville P, et al. *J. Solid State Chem.*, **2008**,**181**:1456-1461

[16]WANG Fei(王飞), TIAN Yi-Guang(田一光), ZHANG Qiao (张乔). *Chinese J. Inorg. Chem.*(无机化学学报), **2014**,**30** (11):2530-2536

[17]Shang M, Liang S, Qu N, et al. *Chem. Mater.*, **2017**,**29**:1813 -1829

[18]Zhou J, Wang Y H, Liu B T, et al. *J. Alloys Compd*, **2009**, **484**:439-443

[19]Chiari G, Calleri M, Bruno E, et al. *Am. Mineral.*, **1975**,**60**: 111-115

[20]Van Uitert L G. *J. Lumin.*, **1984**,**29**:1-9

[21]Dorenbos P. *J. Lumin.*, **2003**,**104**:239-260

[22]Ye S, Liu Z S, Wang X T, et al. *J. Lumin.*, **2009**,**129**:50-54